Advances in Science and Technology Research Journal, 2026, 20(1), 318–339 https://doi.org/10.12913/22998624/211003 ISSN 2299-8624, License CC-BY 4.0 Received: 2025.08.18 Accepted: 2025.09.27 Published: 2025.11.21

Stability of selected open and closed thin-walled beams – numerical analysis

Mikołaj Jan Smyczynski^{1*}, Piotr Paczos¹, Jarosław Pruszyński², Jakub Kasprzak³

- ¹ Institute of Applied Mechanics, Poznan University of Technology, ul. Jana Pawla II 24, 60-965 Poznań, Poland
- ² Zaprom Ltd, Tołcze 3D, 18-106 Tołcze, Poland
- ³ Li-MES Obliczenia i Projektowanie, ul. Milczańska 50/4,61-248 Poznań, Poland
- * Corresponding author's e-mail: mikolaj.smyczynski@put.poznan.pl

ABSTRACT

The paper is devoted to the stability of cold-formed thin-walled profiles. The study includes geometric characteristics of various cross-sections such as closed rectangular profiles and C-shaped profiles with various types of stiffeners. It compares critical forces and stresses of various profile types obtained by finite element method. Results indicate significant differences in critical forces among profiles. The load-bearing capacity of a classic channel-shaped profile modified channel profile and closed rectangular profiles are compared. Profiles with bends show different stability characteristics than standard profiles.

Keywords: thin-walled beam, stability, numerical analysis, rectangular profiles.

INTRODUCTION

The stability of thin-walled beams is an important area of study in structural engineering, particularly due to their susceptibility to buckling under various loads. Therefore, research on these structures is widely described in the literature.

Hancock (1) reviewed and summarised the major research developments in cold-formed steel structures published during 1999-2001. Rhodes and Seah (2) investigated the buckling behaviour of cold-formed edge-stiffened thin-walled steel beams subjected to pure moment loading. Laudiero and Zaccaria (3) presented the numerical calculations of the buckling loads for elastic straight thin-walled beams of open section subjected to any distribution of conservative static loads. Koczubiej and Cichon (4) proposed the finite shell-beam models for static and global stability analysis of thin-walled structures with open cross-sections. Adany and Schafer (5) presented the derivation for a proposed method which can be used for the decomposition of the stability buckling modes of a single-branched open cross-section thin-walled

members into pure bending via finite strip method. Pawlak et al. (6) analysed experimentally and numerically the strength and resistance to loss of stability of thin-walled channel columns. Pawlak et al. (7) presented current state of knowledge of imperfections in thin-walled steel profiles with modified cross-sectional shapes. Mahado (8) analyzed the static non-linear behaviour of thinwalled composite beams with initial imperfections. Magnucka-Blandzi (9) described the effective shaping of cold-formed thin-walled channel beams with double-box flanges subjected to pure bending. Magnucka-Blandzi et al. (10) provided the results of numerical and experimental investigations of buckling problems of cold-formed thinwalled channel beams with double-box flanges in pure bending. Jasion et al. (11) conducted numerical and experimental analysis of buckling and post-buckling behaviour of selected cold-formed C-beams with modified cross-sections and compared them to a classical one. SudhirSastry et al. (12) performed the lateral buckling analysis of cold-formed thin walled channel beams for several combinations of the geometric parameters.

Basaglia et al. (13) and (14) presented the application of the generalised beam theory (GBT) to analyse the local, distortional and global post-buckling behaviour of thin-walled steel frames. Grenda and Paczos (15) investigated the local elastic buckling and limit load of the non-standard thinwalled channel beams subjected to pure bending. Bourihane et al. (16) presented the examination of the stability of thin-walled beams with open section subjected to arbitrary loads. Martins et al. (17) discussed numerical results of the geometrically non-linear behaviour of thin-walled lipped channel columns experiencing local-distortional interaction. Lofrano et al. (18) showed the application of a finite differences procedure to study the buckling of non-trivial equilibrium solutions for open thin-walled beams in a dynamic setting. Chu et al. (19) investigated numerically the local and distorsional buckling behaviour of cold-formed steel zed-section beams subjected to uniformly distributed transverse loads. Li et al. (20) investigated the in-plane behaviour of built-up box beams under pure bending. Pastor and Roure (21) studied numerically open cross-section U- and Omega-beams subjected to pure bending. Horacek and Melcher (22) described the problems of numerical analysis and design of thin-walled steel Sigma beams with circular web holes. Kim et al. (23) analyzed coupled stability of thin-walled composite beams with closed cross-section subjected to various forces based on numerical method. Niu et al. (24) studied effect of moment of inertia on elastic stability of rectangular webs of thin-walled beams under a transverse load. Kesti and Davies (25) assessed the applicability of Eurocode 3 to the prediction of the compression capacity of short columns with different cross-sections due to distortional buckling.

This article presents a strength analysis of thin-walled, open-section channel-shaped profiles subjected to pure bending. These profiles were cold-formed from steel sheets of uniform thickness. Carbon steel profiles require anti-corrosion protection, especially for structures exposed to direct weathering, though not only. Electrogal-vanizing, powder coating, or hot-dip galvanizing are the most common methods used for this purpose. These are well-known, proven technologies that guarantee the durability of steel elements. However, they represent an additional cost in the production of steel structures, especially since in many cases their protection is performed off-site, for example, in galvanizing plants. This increases

not only the production cost but also the time required for completion and the dependence on partners providing such services.

A second disadvantage of steel profiles available on the market is their standardization. They are only available in specific transverse dimensions and wall thicknesses, which impact the entire structure. For example, in the case of large transverse dimensions, thin wall thicknesses are not available. Moreover, for less common dimensions and small quantities, the waiting time for steel profiles can be relatively long.

An alternative to closed and open steel profiles are profiles made from thin sheets of galvanized or powder-coated steel. Such sheets are protected against corrosion in steel mills during production and do not require additional protection if they are cold-processed, for example, by bending or cutting with a guillotine. Thanks to cathodic protection, the cut edge of the sheet is also protected against corrosion.

The aim of the study is to compare the load-bearing capacity of a classic channel-shaped profile and its modifications, which incorporate various types of additional bends in the cross-section. These variants are also compared with a closed rectangular profile, which can also be manufactured from the same sheet metal by appropriate bending and closing the cross-section (Figure 1).

The analysis aims to determine how additional bends (stiffening) and closing the cross-section affect the load-bearing capacity and stiffness of the profile subjected to pure bending. This type of research has significant practical implications in the design of steel structure components, where achieving the highest possible strength with minimal material consumption is crucial.

The study considered the influence of cross-section geometry on critical stress values, as well as the local and global buckling phenomena that can occur in thin-walled cold-formed profiles. Comparative results allow us to assess the effectiveness of individual channel modifications and the feasibility of using closed rectangular cross-sections in the context of increasing the load-bearing capacity of structural elements.

GEOMETRY OF CROSS-SECTIONS AND MATERIAL PROPERTIES

Modern machines for the production of thinwalled cold-formed profiles enable the production

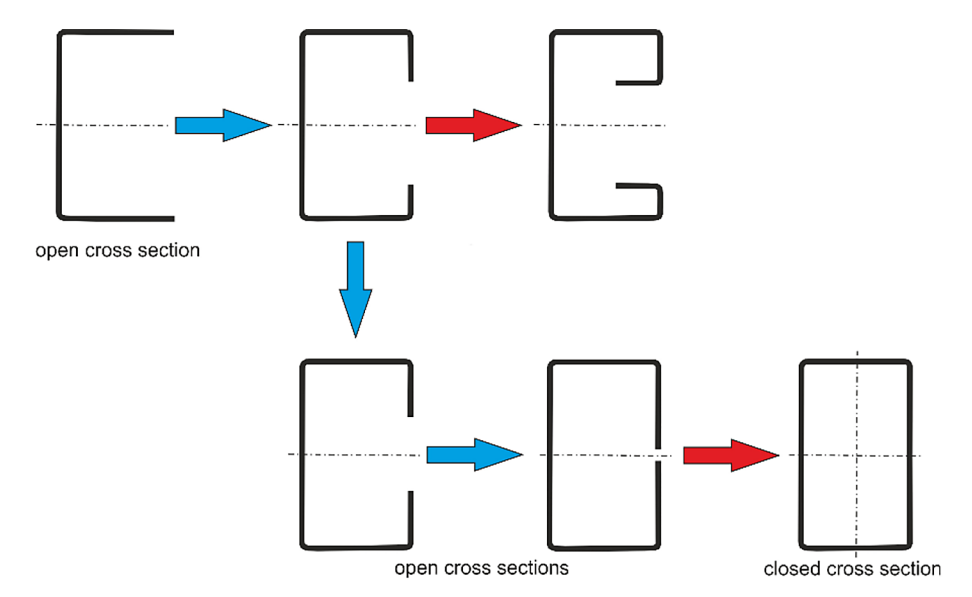


Figure 1. Variants of proposed profiles

of closed profiles as well as profiles of atypical shapes, including C-shaped profiles with various types of stiffeners. They allow for the free determination of the dimensions of the cross-section of the profile and the production of beams with relatively large cross-sectional dimensions, but also small wall thickness.

Geometry of cross-sections

In this study, six different thin-walled profiles made of uniformly thick steel sheet were selected for analysis. these profiles and their dimensions are shown in Figure 2. All profiles were formed using the cold bending method, and their basic form is a channel section modified y the addition of stiffening bends. The final variant analyzed is a closed profile with a rectangular cross-section, also obtained by bending thin sheet metal. This profiles were compared with classical closed rectangular one.

First, the basic geometric characteristics of the cross-sections of the profiles were compared, i.e. surface area (A), moments of inertia (I_x, I_y) and bending strength coefficients (W_x, W_y) . They largely determine the stiffness and strength of the profiles. A comparison of geometric characteristics is presented in Table 1.

The cross-sectional area of the C-shaped profile with a double bend (F) is 38% and 18% larger than the surface area of the classic C-shaped profile (A) and the profile with a single bend (B), respectively. The double bend increases the main moments of inertia of the profile, however, in the case of the larger one I to a lesser extent than

would result from the increase in surface area, because "only" by 26% and 10% in relation to the profile with a single bend (B) and the classic C-shaped profile (A) without bends. In the case of the smaller of the main moments of inertia I_y , this increase is 93% and 15%, respectively.

This analysis of the geometric data indicates that adding bends and closing the cross-section has a positive effect on both the moment of inertia about the bending axis I_x and the strength modulus W_x . An increase in these parameters indicates greater stiffness and load-bearing capacity of the profiles subjected to bending. However, it should be noted that these changes are not linear – some profiles with larger cross-sectional areas show only a slight improvement in stiffness parameters, which may indicate suboptimal geometry in terms of material efficiency.

Material properties

The material properties of DC01 steel with a nominal yield strength (fy) of 295 MPa were considered. The stress-strain behaviour of DC01 sections in flat and corner regions was determined using the material models recommended by Zhao et al. (26) and Gardner and Yun (27), respectively. To obtain a true stress-strain curve, the engineering stress-strain curve was transformed using the following equations:

$$\sigma_{true} = \sigma (1 + \varepsilon) \tag{1}$$

$$\varepsilon_{true} = ln (1+\varepsilon) - \frac{\sigma_{true}}{E}$$
 (2)

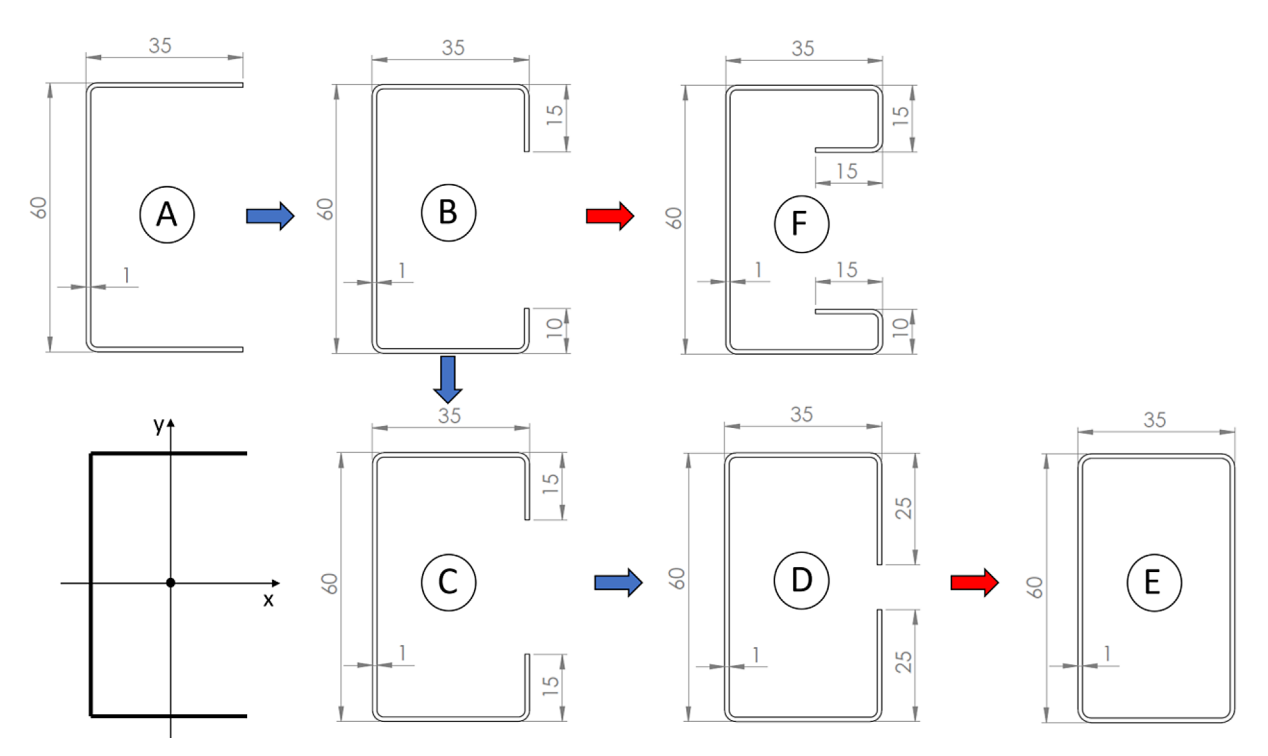


Figure 2. Analyzed coss-sections and their dimentions

Table 1. Summary of geometrical characteristics of the cross-sections of channel profiles shown in Figure 2

Profile	А	I _x	I _y	W _x	W _y
	cm ²	cm ⁴	cm ⁴	cm ³	cm ³
А	1.26	7.57	1.62	0.2523	0.0476
В	1.48	8.65	2.71	0.2878	0.0805
С	1.54	8.81	2.93	0.2937	0.0873
D	1.73	9.03	3.66	0.3010	0.1097
E	1.82	8.96	3.94	0.2987	0.1185
F	1.74	9.53	3.13	0.3176	0.0935

where: E defines the elastic modulus, σ is the engineering stress, ε is the engineering strain, σ_{true} is the true stress and ε_{true} is the true strain.

The cross-section of the CFS closed built-up beam section investigated in this work is unique, combining the benefits of an 'I' section and a closed-box section. The built-up section is constructed from two identical plain channels placed back-to-back with space between them, which can be referred to as web channels, and fastened together at the top and bottom by two inverted plain channels, which can be referred to as flange channels. Two rows of self-driving screws were used to connect the web of flange channels and flange of web channels at regular intervals. Four flat samples and four cut from the corner of a beam were tested.

The average test results for the 8 tests performed are presented in Table 2 and Figure 3.

STABILITY OF THIN-WALLED PROFILES

Thin-walled profiles used in various types of structures transfer both bending and compressive loads. Due to their shape, channels are mainly used to transfer bending loads. In such a case, they are exposed to loss of stability:

- local due to buckling of the upper (compressed) shelf (Figure 4),
- distortion caused by the change in the crosssectional shape of the profile, i.e. the collapse of the upper/compressed flange,
- global due to torsional or flexural-torsional buckling (Figure 5).

Stool grade	Parameter	E	f _y	$f_{_{ m u}}$	$\boldsymbol{arepsilon}_{y}$	$\boldsymbol{arepsilon}_{\mathrm{u}}$
Steel grade Parameter	[GPa]	[N/mm ²]	[N/mm ²]	[%]	[%]	
DC 01	Flat	221	295	360	2.01	22.62
EN 10139	Corner	185	309	354	1.77	19.27
(1.0330)						

Table 2. Summary of flat and corner material properties for DC01 steels employed in parametric studies

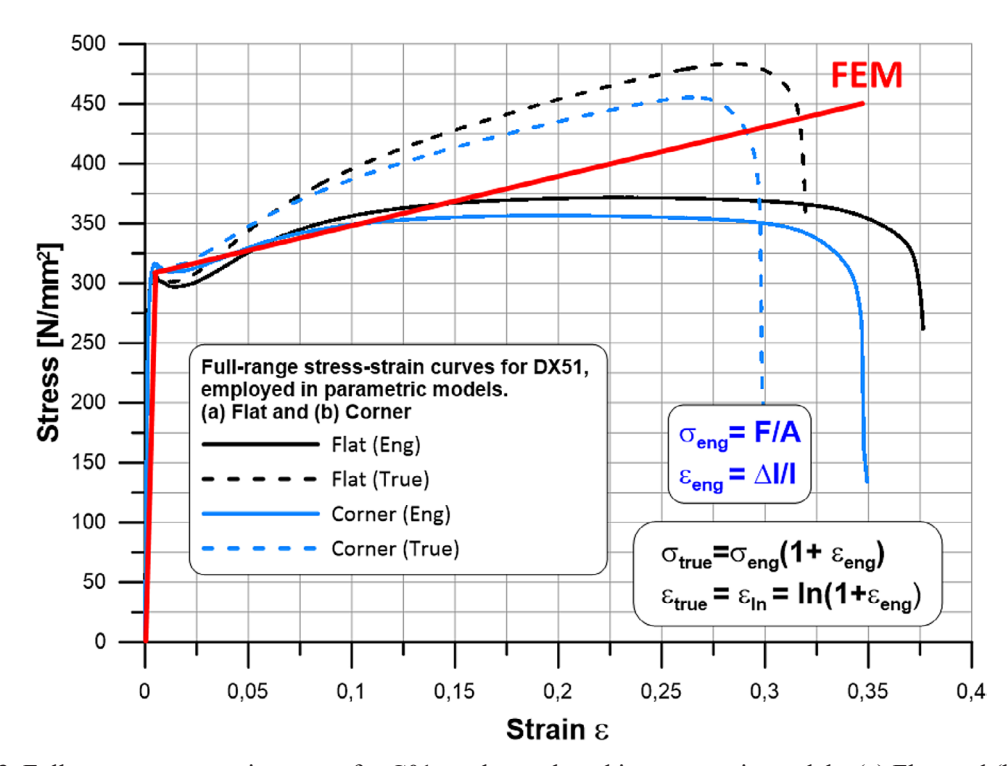


Figure 3. Full-range stress-strain curves for C01 steels employed in parametric models. (a) Flat; and (b) Corner

In order to estimate the influence of bends on the stability of channel profiles, the critical stress values of the profiles shown in Figure 2, in the pure bending state were compared.

As mentioned earlier, the cross-sectional shape of thin-walled, open profiles can be deformed during bending and the results obtained using classical beam theory may be subject to error. For this reason, in this study, the finite element method and CAE (Computer Aided Engineering) SolidWorks Simulation software integrated with the popular CAD (Computer Aided Design) SolidWorks system was used to analyze beams.

Due to the fact that the wall thickness is small in relation to the cross dimensions of the profiles, triangular shell finite elements of the second order were used to model them. They are built from three parabolic edges and six vertices. The distribution of displacements inside such elements is described by a quadratic function, and the distribution of stresses/strains by a linear function. An example finite element mesh of a channel profile with two bends of length $L=60\,\mathrm{cm}$ is shown in Figure 6. The maximum element size in this case is 5 mm.

As mentioned above, beams in pure bending were analyzed to avoid the torsion effect that occurs during bending of open profiles loaded with a transverse force (concentrated, uniformly distributed, etc.). It was assumed that the profiles are supported by sliding hinge. For this reason, vertical and horizontal displacements in the plane perpendicular to the beam axis were blocked at both ends of the profile (Figure 7, arrows marked in green). Additionally, displacements in the direction of the beam axis were blocked along the central edge of the web (Figure 7, arrows marked in blue).

Beams in pure bending are loaded at both ends with bending moments of the same

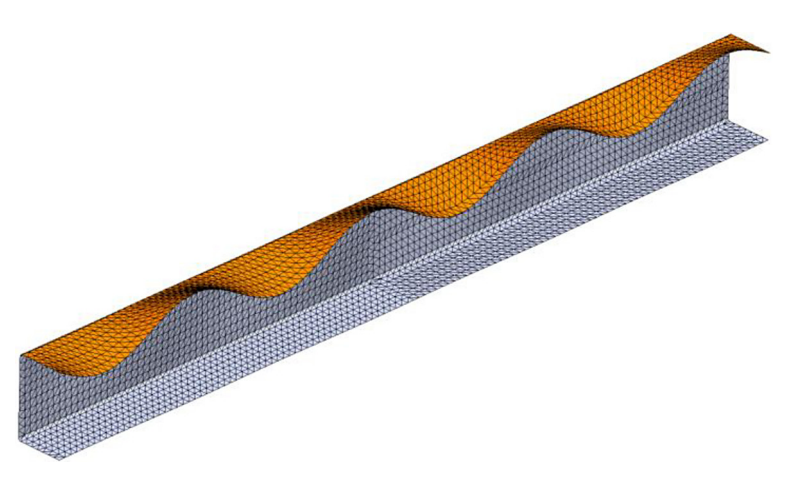


Figure 4. Classical channel section in pure bending: local buckling of the upper (compressed) flange



Figure 5. Classical channel section in pure bending: global (torsional) buckling

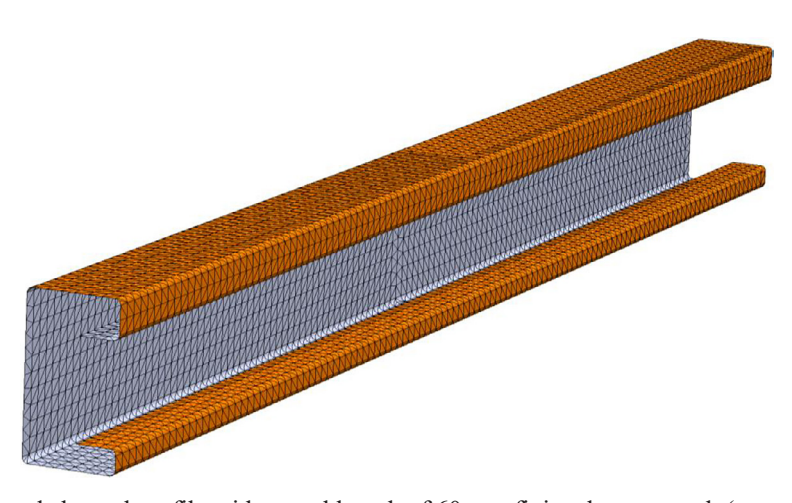


Figure 6. Double-bend channel profile with a total length of 60 cm: finite element mesh (max. element size 5 mm)

magnitude and opposite directions. In the numerical model, bending moments were modeled using pressure acting in the direction of the beam axis, changing linearly from zero in the neutral plane to $+\sigma_{max}$ in the upper flange and $-\sigma_{max}$ in the

lower flange (Figure 8). In reality, the profiles B and F are not symmetrical. However, their axis/neutral plane is offset from the middle plane by 0.01 and 0.06 mm, respectively. These are negligibly small values, constituting less than 0.1%

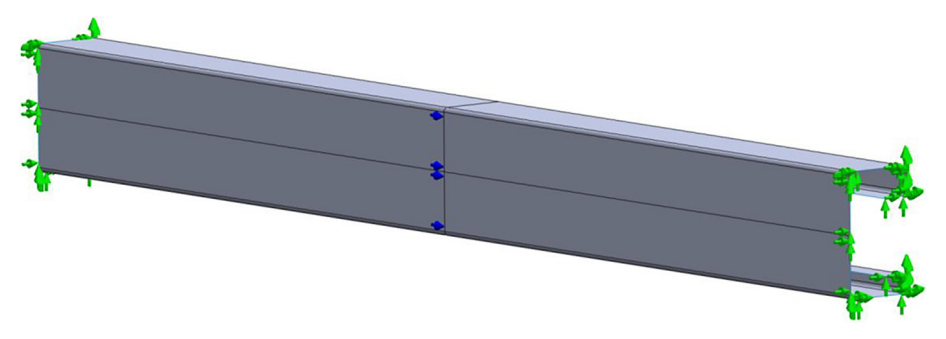


Figure 7. Boundary conditions of a beam supported by a sliding hinge at both ends

of the height of the entire profile. The following boundary conditions were applied to numerical models of beams. At both ends of beams, displacements in plane perpendicular to the beam axis were locked (uy = uz = 0). Displacements parallel to the beam axis were locked along the centre of the web. The profile loading scheme is shown in Figure 9. The red arrows visible on it indicate the direction and sense of the load. The arrows closer to the neutral plane are proportionally smaller.

The optimal size of finite elements was determined by performing a convergence analysis. Figure 10 shows a graph defining the relationship between the maximum size of finite elements and critical stresses. Approximating this relationship using a linear function, the equation of which is shown in Figure 10, it is possible to estimate the limit to which the value of critical stresses tends with the reduction of the size of finite elements to zero. It is 105 MPa and is only 0.5% smaller than the values of critical stresses

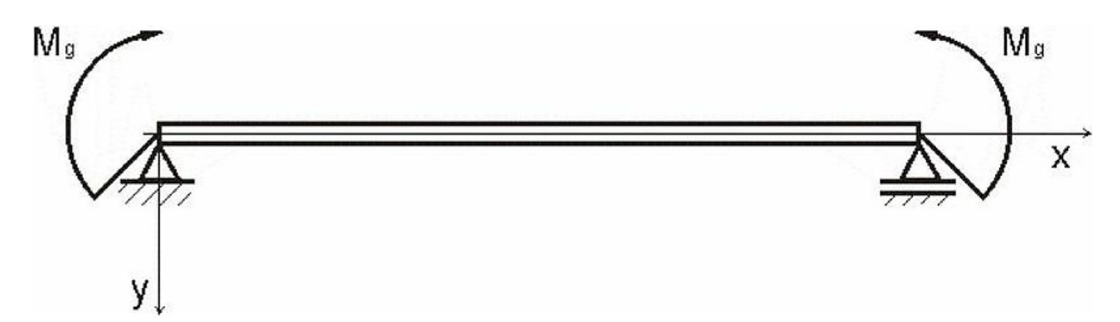


Figure 8. Clean bending: scheme

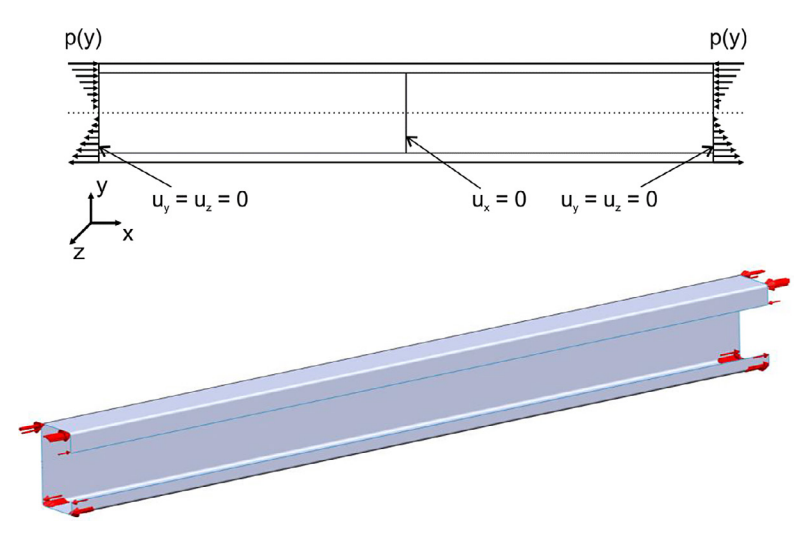


Figure 9. Beam load scheme (pressure acting in the beam axis applied to its ends and changing linearly)

determined using finite elements with the maximum size of 5 mm.

A similar analysis was performed for the maximum deflection of a profile with two bends with a total length of 60 cm, in which the maximum bending stresses are $\sigma_{max} = 100$ MPa (Figure 11). In this case, the relationship between the maximum size of finite elements and the maximum beam deflection was approximated by a quadratic function, the equation of which is shown in Figure 11. The value to which the maximum beam deflection tends with the reduction of the size of finite elements is 1.0527 and is practically the same as the beam deflection determined using finite elements with a maximum size of 5 mm.

For the above reasons, a maximum finite element size of 5 mm was assumed in all presented analyses.

In order to estimate the influence of bends on the stability of profiles, the values of critical stresses of beams in the state of pure bending were compared, presented in Figure 2. Both linear and nonlinear analysis, taking into account geometric nonlinearities, were used for this purpose. The obtained results are presented in Figure 12 and in Table 3.

Classical channels without bends are susceptible to local loss of stability (corrugation of the upper/compressed flange, Figure 13). This can be observed for beams 150 cm long and shorter.

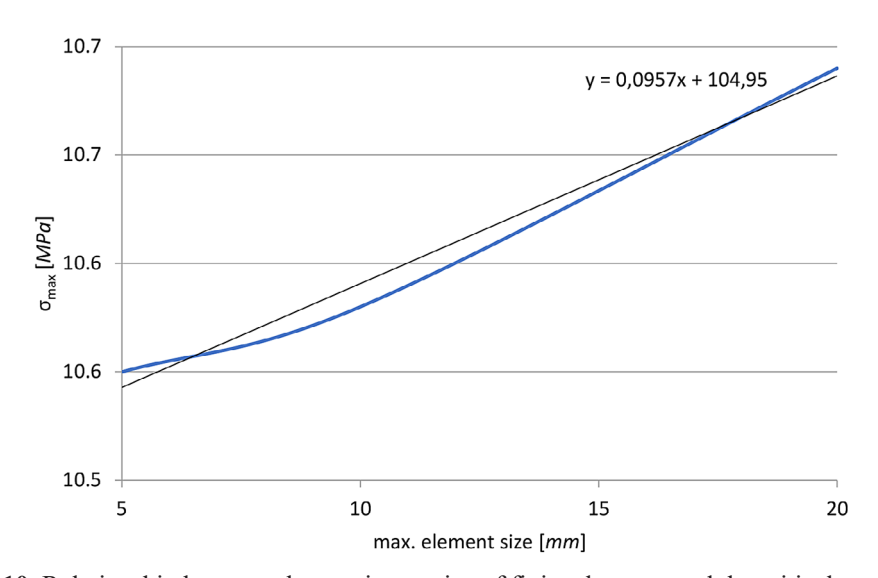


Figure 10. Relationship between the maximum size of finite elements and the critical stress value for a double-bend C-profile with a total length of $L=60~\mathrm{cm}$

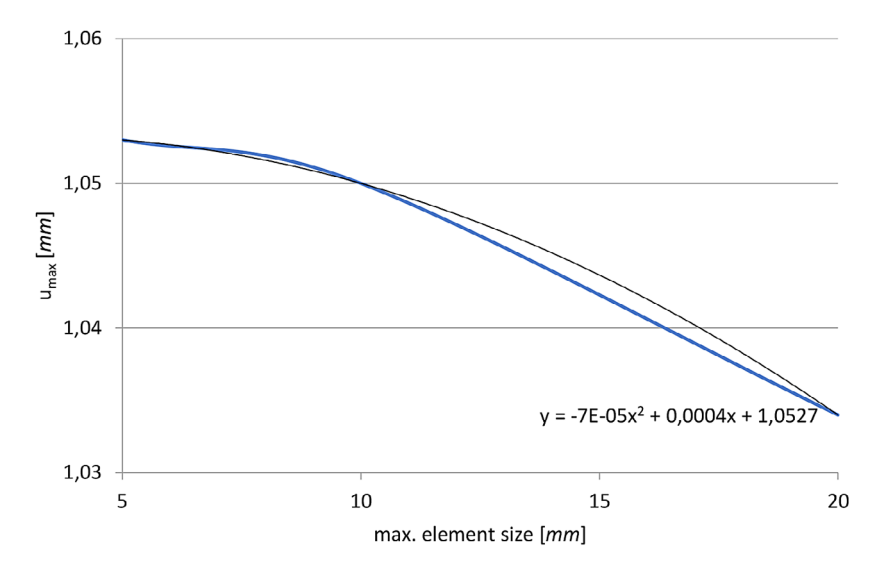


Figure 11. Relationship between the maximum finite element size and the maximum deflection of a double-bent channel profile with a total length of L = 60 cm, $\sigma_{max} = 100$ MPa

Moreover, in the range of 60150 cm, critical stresses are practically independent of the beam length. In other words, shortening the beam, e.g. the distance between supports does not increase its strength. In the case of longer beams, the loss of stability occurs due to torsional and distortional buckling (Figure 14, 15). The buckling moment can be clearly seen in the graphs showing the relationships between deflection and load and stresses presented in Figure 16 and Figure 17. In the first case (Figure 16), a straight line break is clearly visible at the moment of buckling. The relationships between deflection and stresses at the moment of buckling are no longer monotonic (Figure 17).

The critical stresses range from 152 MPa for short beams to 77 MPa for long 240 cm beams. They are 46–76% lower than the yield strength of the popular S280 GD steel used for the production

of unusual thin-walled cold-formed profiles ($\sigma a = 280 \text{ MPa}$). Therefore, it is not the strength of the material that limits the load-bearing capacity of the beams but their stability.

The inserting of a single stiffening bend of the flange eliminates the problem of local buckling in short beams. The determined values of critical stresses for channels 150 cm long and less exceed the yield strength. They are therefore of purely theoretical importance, because in such a case, to determine their exact value, a nonlinear/plastic material model would have to be used. However, this goes beyond the scope of this study, in which, in accordance with engineering practice, the work of the structure in the elastic range was assumed. In the case of long channels with a single bend, critical stresses are 125–241 MPa, which is 14–55% lower than the yield strength of DC01 steel. As before, the load-bearing capacity of these

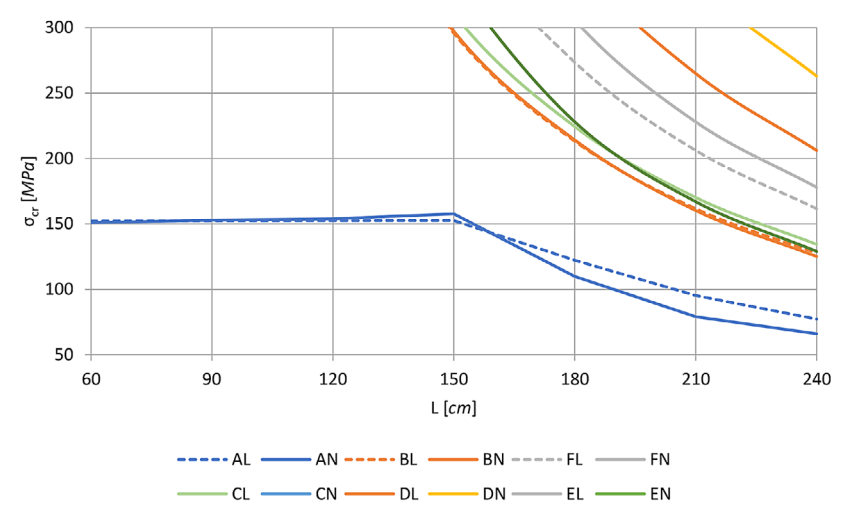


Figure 12. Relationship between critical stresses and beam length; L – linear analysis; N – non-linear analysis

Table 6. Citizent Stress variety of chainsel central [111 a]								
Profiles	L [cm]	60	90	120	150	180	210	240
A	σ _{cr, linear}	152	152	152	153	122	95	77
	σ _{cr, non-linear}	151	153	154	158	110	79	66
В	σ _{cr, linear}	786	698	439	296	213	162	128
	σ _{cr, non-linear}	719	760	445	297	214	160	125
F	σ _{cr, linear}	910	889	565	380	274	206	162
	σ _{cr, non-linear}	724	674	622	432	306	228	178
С	σ _{cr, linear}	786	717	458	311	224	170	134
	σ _{cr, non-linear}	728	760	486	358	218	167	129
D -	σ _{cr, linear}	710	711	712	490	352	265	206
	σ _{cr, non-linear}	768	704	654	550	430	334	263
E -	σ _{cr, linear}	856	856	854	850	845	838	831
	σ _{or non linear}	861	849	853	860	843	840	834

Table 3. Critical stress values of channel beams [MPa]

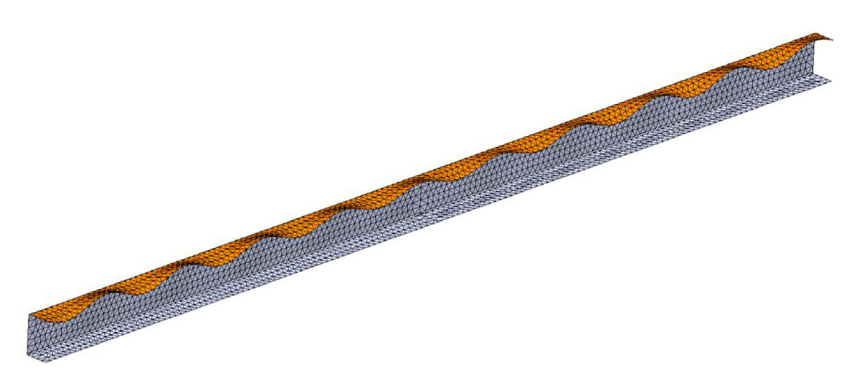


Figure 13. Buckling mode of a classic channel section L = 150 cm, $\sigma_{cr} = 153$ MPa (linear analysis)

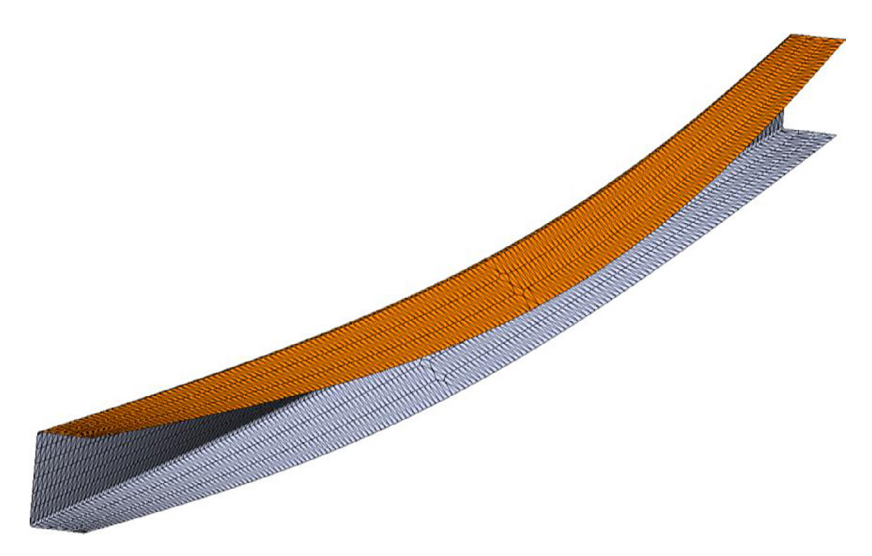


Figure 14. Buckling mode of a classic channel section L = 180 cm, $\sigma_{cr} = 122$ MPa (linear analysis)

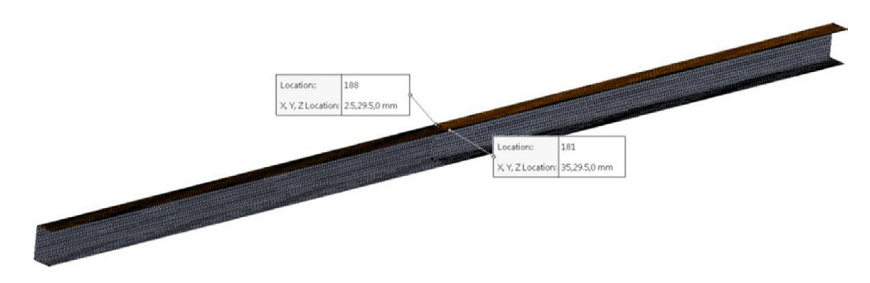


Figure 15. Classic channel section L = 180 cm: points where the relationship between deflection and stress/load was determined

beams is limited by torsional buckling (Figure 18), not by the strength of the material.

In the case of stiffening the channel edge with a double bend, the critical stress values increase by more than 40% compared to beams with a single bend (with only an 18% increase in mass). Moreover, only beams longer than 180 cm undergo buckling in the elastic range. The critical stresses of the longest of the considered beams (L = 240 cm) are 36% lower than the yield strength of DC01 steel.

RECTANGULAR PROFILES

Thin-walled steel beams/profiles with open and closed cross-sections are popular structural elements. These include rectangular beams. Carbon steel profiles require anti-corrosion protection, especially for structures exposed to direct weathering, though not only. Electrogalvanizing, powder coating, or hot-dip galvanizing are the most common methods used for this purpose. These are well-known, proven technologies that

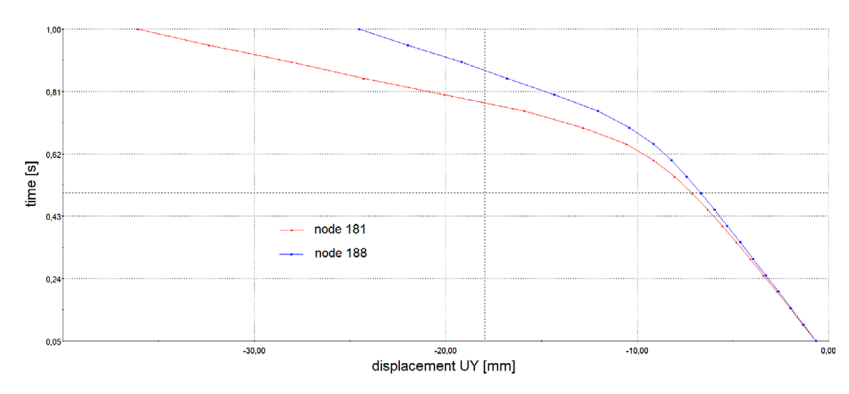


Figure 16. Classic channel section L = 180 cm: relationship between deflection and load at points shown in Figure 16 (1.00 = σ_{max} = 200 MPa)

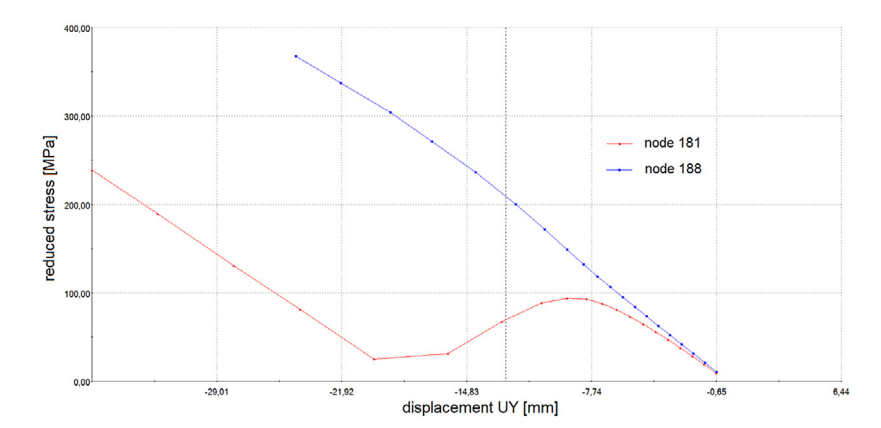


Figure 17. Classic channel section L = 180 cm: relationship between deflection and stresses at the points shown in Figure 16

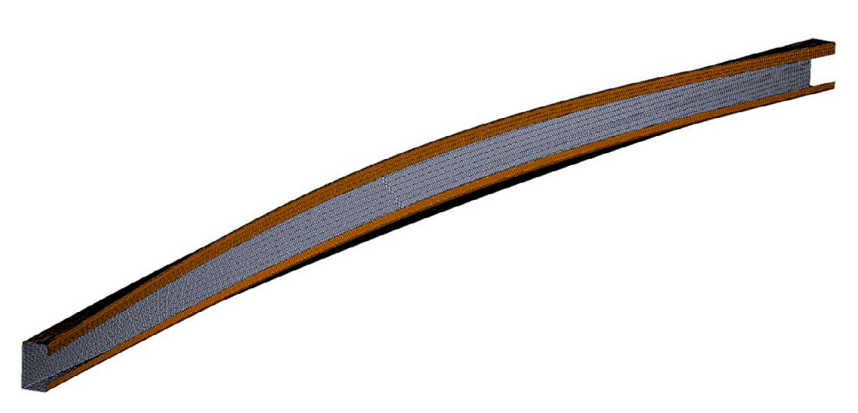


Figure 18. Buckling mode of a single-bend channel section L = 210 cm, $\sigma_{cr} = 160$ MPa (linear analysis)

guarantee the durability of steel elements. However, they represent an additional cost in the production of steel structures, especially since in many cases their protection is performed offsite, for example, in galvanizing plants. This increases not only the production cost but also the time required for completion and the dependence on partners providing such services.

A second disadvantage of steel profiles available on the market is their standardization. They are only available in specific transverse dimensions and wall thicknesses, which impact the entire structure. For example, in the case of large transverse dimensions, thin wall thicknesses are not available. Moreover, for less common dimensions and small quantities, the waiting time for steel profiles can be relatively long.

An alternative to closed and open steel profiles are profiles made from thin sheets of galvanized or powder-coated steel. Such sheets are protected against corrosion in steel mills during production and do not require additional protection if they are cold-processed, for example, by bending or cutting with a guillotine. Thanks to cathodic protection, the cut edge of the sheet is also protected against corrosion.

It is worth noting that today's advanced and innovative machines for the production of thin-walled cold-formed profiles enable the production not only of open profiles, such as angles, channels, or Z-sections, but also of closed profiles, such as those with a rectangular cross-section. These machines allow for the free definition of the profile's cross-section dimensions and the production of beams with relatively large cross-sections but also with a thin wall thickness.

Geometry of rectangular profiles

In this study, two types of rectangular profiles are considered, as shown in Figure 19. These proposed profiles are cold-formed from steel sheets and they are compared with their classic counterparts, as shown in Figure 20. It should be noted, that Profile 1B is not available as standard.

First, the basic geometrical characteristics of the cross-sections of the profiles were compared, i.e. the surface area, moments of inertia and bending strength coefficients (Table 4). They largely determine the stiffness and strength of the

profiles. A comparison of geometrical characteristics is presented in Figure 21.

In addition, Figure 21 shows the influence of the height of Profile 1 on the difference between the geometric characteristics. It can be seen that in the case of the surface area and the main moments of inertia, the difference between the standard rectangular profile and the profile made of sheet metal decreases with the increase in the profile height. The greatest differences occur in the case of the main moment of inertia I_{x1} (even 19% for a profile with a height of H = 60 mm) and the cross-sectional area A (even 14% for a profile with a height of H = 60 mm). These differences decrease to 12 and 5%, respectively, for profiles with a height of H = 200 mm. A similar relationship, i.e. a decrease in the difference between the characteristics with the increase in the profile height, also applies to the second main moment of inertia Iy1, but in this case the differences between the moments of inertia are small and are in the range of 1.3–0.5%.

Stability of rectangular profiles

Thin-walled profiles used in various types of structures carry both bending and compressive loads. In the case of compression, the profiles may lose stability due to buckling. In order to estimate the influence of production technology on the stability of profiles, the forces and critical stresses for profiles supported by

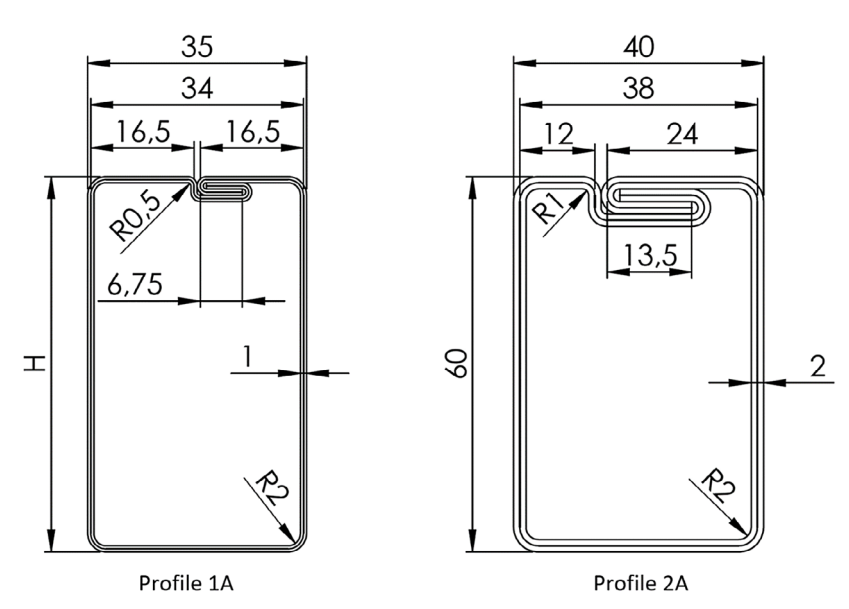


Figure 19. Cross-section of rectangular profiles made of steel sheet by cold bending (H = 60 / 80 / 100 / 120 / 200)

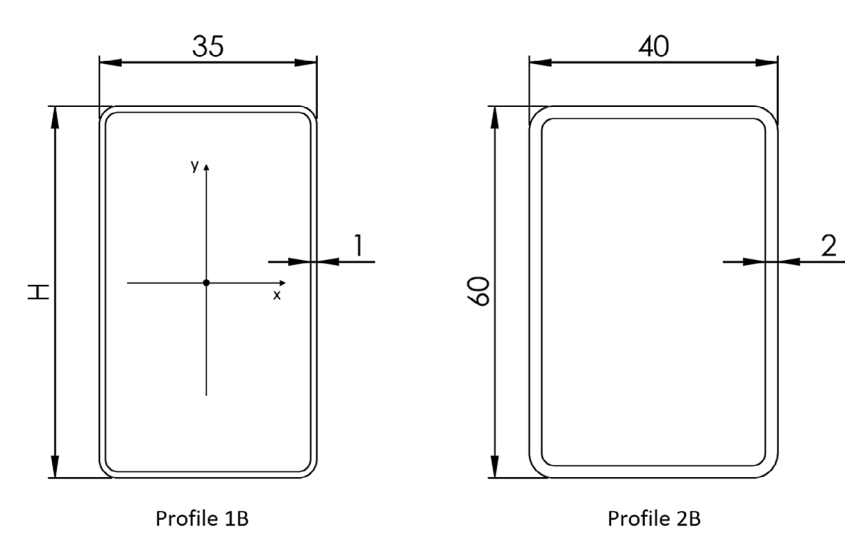


Figure 20. Standard rectangular profiles (H = 60 / 80 / 100 / 120 / 200)

Table 4. Summary of geometrical characteristics of standard and cold-formed rectangular cross-sections

Profil	А	I _x	l _y	W _x	W _y
Piolii	cm ²	cm⁴	cm ⁴	cm ³	cm ³
1A H = 60 mm	1.82	8.96	3.94	2.99	2.25
1B H = 60 mm	2.07	10.66	3.99	3.19	2.22
Difference	13.7%	19.0%	1.3%	6.9%	-1.5%
1A H = 80 mm	2.22	18.15	5.09	4.54	2.91
1B H = 80 mm	2.47	21.38	5.15	4.87	2.88
Difference	11.3%	17.8%	1.2%	7.3%	-1.1%
1A H = 100 mm	2.62	31.77	6.25	6.35	3.57
1B H = 100 mm	2.87	37.04	6.30	6.83	3.52
Difference	9.5%	16.6%	0.8%	7.6%	-1.5%
1A H = 120 mm	3.02	50.62	7.41	8.44	4.23
1B H = 120 mm	3.27	58.45	7.46	9.06	4.19
Difference	8.3%	15.5%	0.7%	7.4%	-1.0%
1A H = 200 mm	4.62	194.39	12.03	19.44	6.87
1B H = 200 mm	4.87	217.55	12.09	20.70	6.83
Difference	5.4%	11.9%	0.5%	6.5%	-0.6%
2A	3.74	18.41	9.83	6.14	4.92
2B	4.77	23.41	10.13	6.61	4.97
Difference	27.5%	27.2%	3.1%	7.8%	1.0%

sliding hinge and subjected to axial compression were compared.

For standard thin-walled profiles, the critical force for compressed bars can be determined using the well-known formula, the so-called Euler solution, presented below:

$$F_{cr} = \pi^2 \times E \times I_{\min} \div L^2 \tag{3}$$

where: F_{kr} – critical force, E = 210 GPa is the Young's modulus of steel, $I_{min} = \min (I_1, I_2)$ – the smaller of the main moments of

inertia of the cross-section of the profile, L – reduced length of the profile.

In the case of thin-walled profiles cold-formed and made from a single sheet, this formula gives only approximate results because it does not take into account phenomena occurring at the joint of the profile walls (bends). Moreover, it only concerns global buckling, completely omitting local, distortional buckling, or interactions between different types of buckling. Therefore, in order to determine the critical load values, the finite element method and the CAE software SolidWorks Simulation were used, as in the previous chapter.

Due to the fact that the wall thickness of the profiles is small in relation to the cross dimensions of the profiles, triangular shell finite elements of the second order were used to model the profiles, as in the previous chapter. An example finite element mesh of profile 2A is shown in Figure 22. The maximum element size in this case is 5 mm. This mesh consists of 12,420 vertices and 6.105 elements.

The optimal size of finite elements was determined by conducting a convergence analysis. Figure 23 shows a graph defining the relationship between the maximum size of finite elements and the critical force. Approximating this relationship using a linear function, the equation of which is shown in Figure 23, it is possible to estimate the limit to which the value of the critical force tends with the reduction of the size of the elements to zero. It is 62.055 kN and is only 0.16% smaller than the value of the critical force determined using finite elements with a maximum size of 5 mm. Due to the fact that the difference between these forces

is so small, in all presented ones the maximum size of finite elements equal to 5 mm was assumed.

First, the critical force values for standard rectangular profiles determined using formula (1) and the finite element method were compared. The results obtained for profile 2A, depending on its total length, are presented in Table 5. With the exception of a very short beam of 60 cm, the differences between the analytical and numerical solutions amount to only a few percent and decrease with the length of the profile. The large difference between the results for the 60 cm long beam results from the fact that in this case only the profile wall buckles (local buckling, Figure 24). It should be noted that the results contained in Table 5 and marked in gray have only theoretical significance, because the obtained critical stress values exceed the yield strength. In other words, in this case the profile buckles only in the plastic range and its correct modeling would require the use of appropriate material models.

Then, the critical forces and stress values were compared between a standard rectangular profile $60 \times 40 \times 2$ (Profile 2B) and a cold-formed profile (Profile 2A). In the latter case, two extreme situations were considered:

- no bond (weakly tightened bend, possibility of sheet slipping out),
- full bond (tightly tightened bend, no possibility of sheet slipping out or moving).

The comparative analysis was limited only to the linear-elastic range, i.e. profiles with a length of 150 to 240 cm. The calculated critical forces are shown in Figure 25. Depending on the assumption made regarding the bend

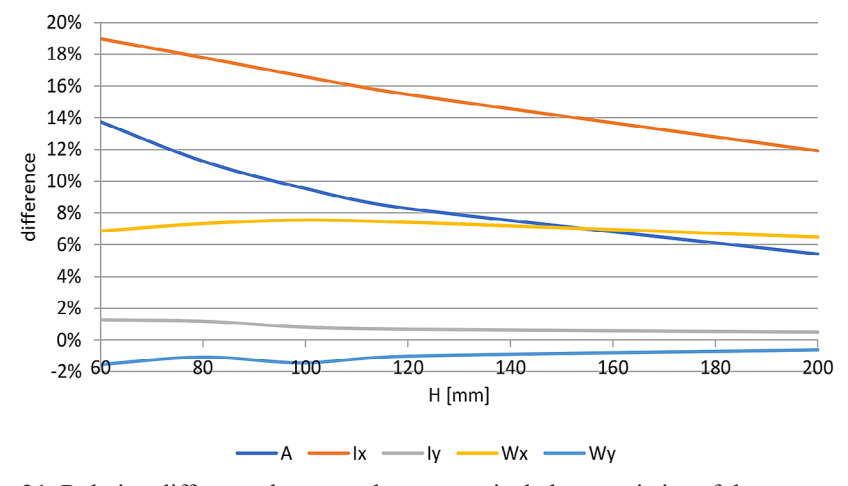


Figure 21. Relative difference between the geometrical characteristics of the cross-sections of profiles 1A and 1B depending on the profile height

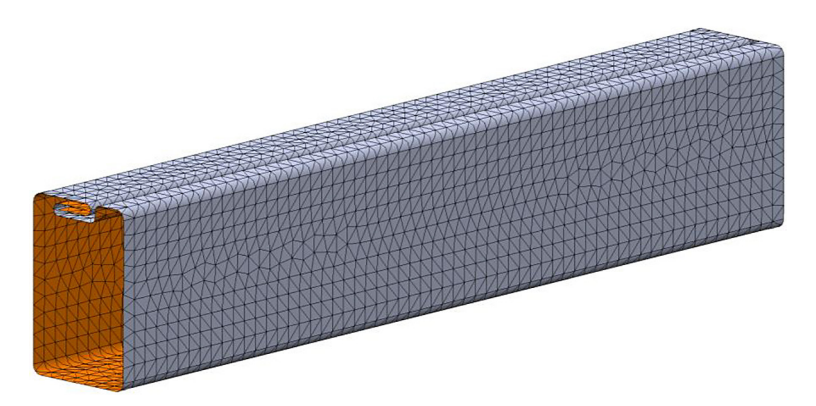


Figure 22. The half of profile 2A with a total length of 60 cm: Finite element mesh (max. element size 5 mm)

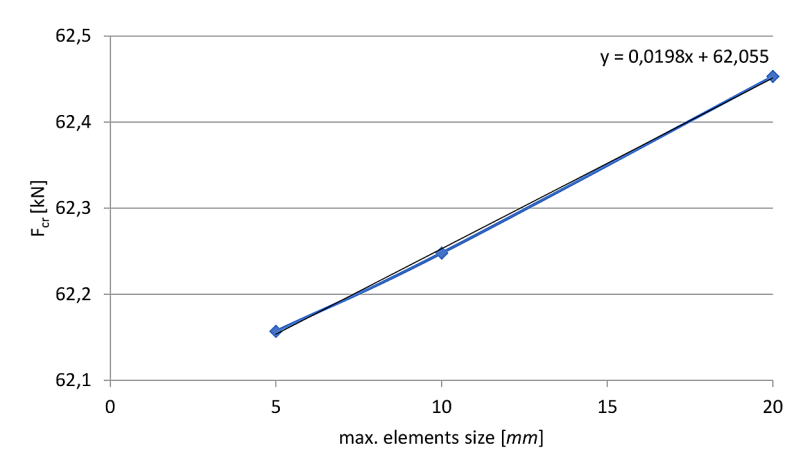


Figure 23. Relationship between the maximum size of finite elements and the critical force value for profile 2A with total length L = 1.8 m

strength (no bond or full bond), the critical force of profile 2A is 5% lower or 3% higher than the critical force of profile 2B. These differences are not dependent on the length of the profile. Moreover, due to the fact that they are small, it can be stated that cold-formed Profile 2A has a similar resistance to buckling in axial compression to a standard rectangular profile. On the other hand, the way the bend is made is important and the stronger and more precisely it is made, the higher the critical force will be. The differences between the critical stresses are approx. -24% in the case of no bond at the bend and approx. -11.4% in the case of taking into account full bond at the bend of profile 2A. This means that regardless of the bending model and the quality of its execution, the critical stresses of the coldbent $60 \times 40 \times 2$ profile are lower than the stress of a standard rectangular profile compressed axially. This is not so much due to the lower critical force of the cold-formed profile as to the larger cross-sectional area (Figure 26).

A similar comparative analysis was carried out for profiles 1A and 1B. Figure 27 shows a comparison of the critical forces of profiles 1A and 1B with a height of H = 60 mm. Similarly to the previous case, the critical force of the coldformed profile can be up to 14% lower than the critical force of a standard rectangular profile. This applies to a situation in which the bend is so weak that profile 1A can be treated as open. In the case of a well-made bend, the critical force of the cold-formed profile is, in the considered length range, approx. 1% higher than the force of a standard closed profile. The buckling forms of profiles 1A and 1B with a height of H = 60 mmand length L = 150 cm are shown in Figure 28 and Figure 29. In the case of failure to take into account the bond at the bend of profile 1A, the compressed beam not only bends but also twists, i.e. it undergoes lateral warping. In the case of a closed profile and taking into account the full bond at the bend, both profiles only undergo flexural buckling. Since the cross-sectional area of profile 1A is larger than that of profile 1B, the critical

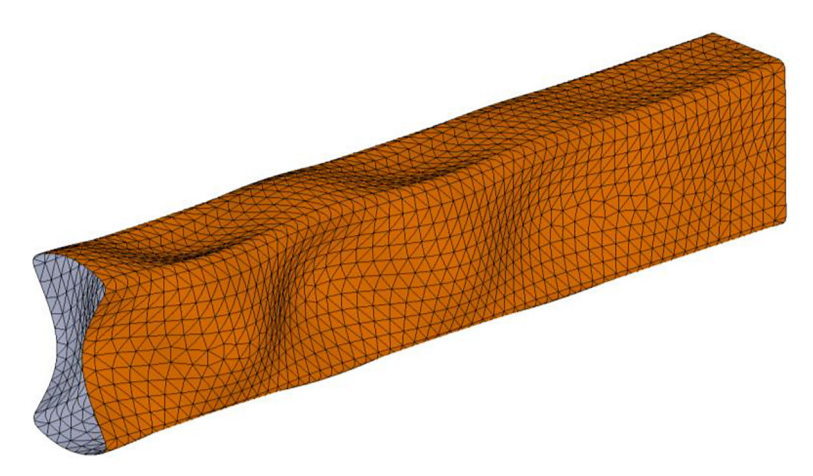


Figure 24. Profile 2B, L = 60 cm: buckling shape (local buckling)

Table 5. Comparison of critical stresses of profile 2B determined analytically and using the finite element method

L	$\sigma_{ m cr.t}$	$\sigma_{_{ m cr.MES}}$	Difference $\sigma_{cr.t}$ / $\sigma_{cr.MES}$ -1
ст	MPa	MPa	-
60	1 513	1112	36.1%
72	1 051	1000	5.1%
75	968	925	4.7%
90	673	651	3.3%
120	378	371	2.0%
150	242	239	1.5%
180	168	166	1.2%
210	124	122	1.0%
240	95	94	0.9%

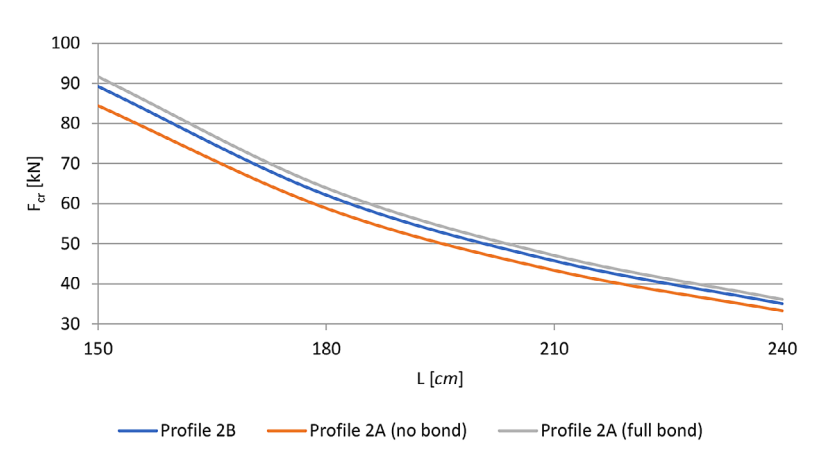


Figure 25. Comparison of critical forces of profiles 2A and 2B

stresses of the cold-formed profile are lower by 11 and 24%, depending on whether the bond at the bend is taken into account or not.

Similar dependencies can be observed in profiles 1A and 1B with a height of 80 mm (Figure 30). However, this only applies to appropriately long profiles. In the case when their length

is 120–150 cm, the walls of profiles 1A and 1B are subject to folding, i.e. local buckling (Figure 31 and Figure 32). Then, regardless of the way of modeling the bend (without bond or with bond), the critical force of the cold-formed profile is 12–13% higher than the critical force of the standard rectangular profile. Longer profiles (≥

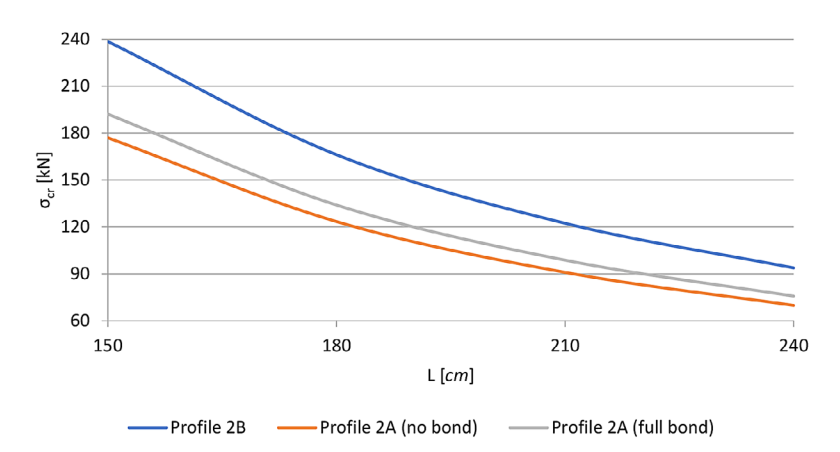


Figure 26. Comparison of critical stresses of profiles 2A and 2B

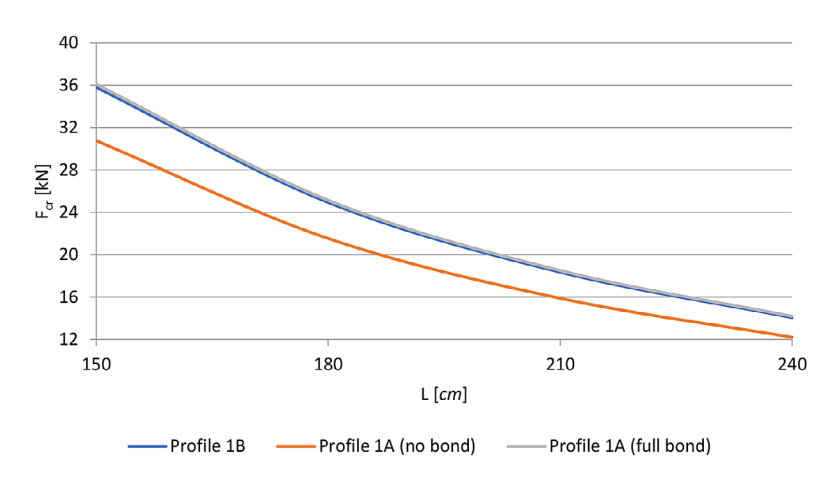


Figure 27. Comparison of critical forces of profiles 1A and 1B, H = 60 mm

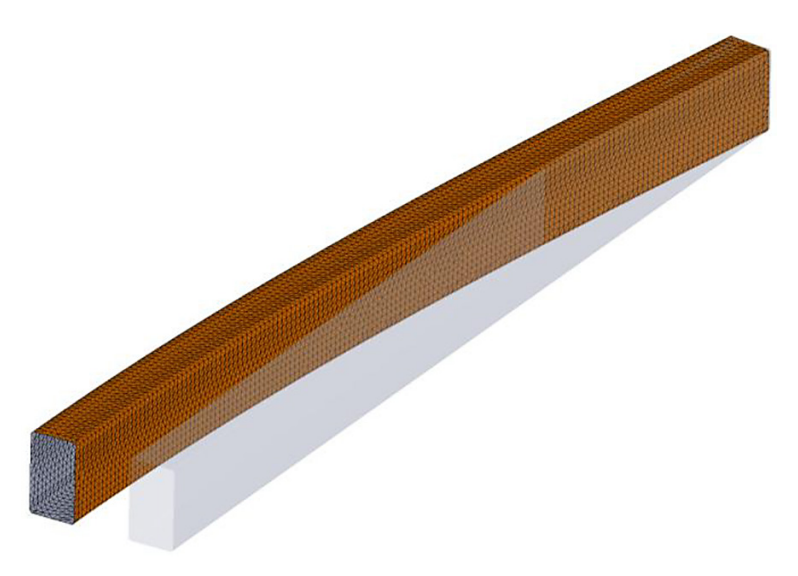


Figure 28. Profile 1B with height H = 60 mm and length L = 150 cm (only half of the profile is shown): buckling shape ($F_{cr} = 35.8$ kN)

180 cm) are subject to flexural buckling (profiles 1A with bond and 1B) or buckling (profile 1A without bond). Then the critical force of profile 1A is comparable to the critical force of profile

1B if the bend is made correctly and prevents the sides of the profile from separating. Otherwise, it is about 17% lower. It should be noted that the transition from local buckling to lateral torsional

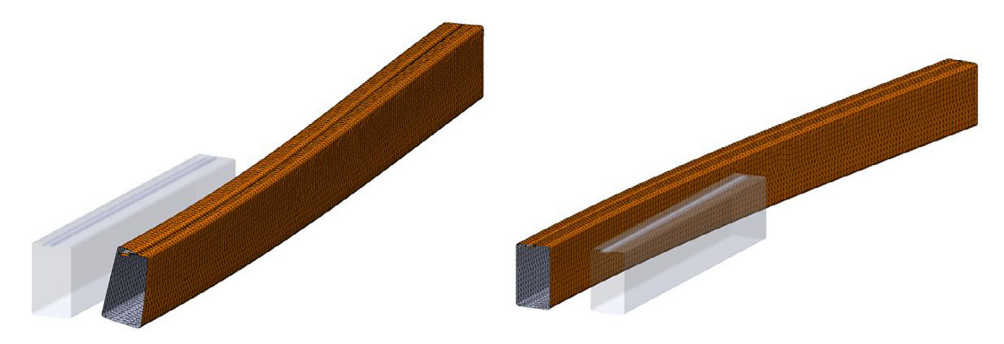


Figure 29. Profile 1A with height H = 60 mm and length L = 150 cm (only half of the profile is shown): buckling form with no bond at the bend ($F_{cr} = 30.8 \text{ kN}$) and with full bond at the bend ($F_{cr} = 36.1 \text{ kN}$)

buckling (global buckling) is "smooth", which is confirmed by the observation of interactions between different buckling modes in profile 1A with a height of 80 mm and length L = 150 cm, in which the bond at the bend was not taken into account (Figure 33).

In higher profiles 1A and 1B, local buckling, i.e. corrugation of the profile walls, concerns increasingly longer beams. Moreover, the critical force in this case does not depend on the length of the profile, but only on its height (Figure 34, Figure 35). The relationship between the height

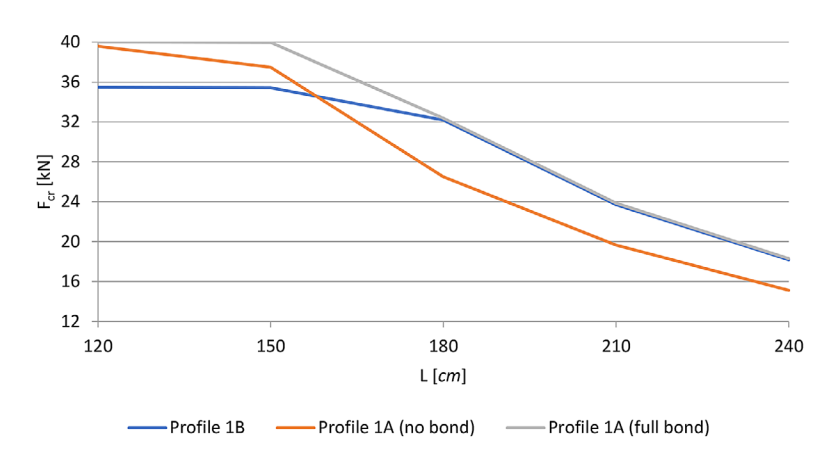


Figure 30. Comparison of critical forces of profiles 1A and 1B, H = 80 mm

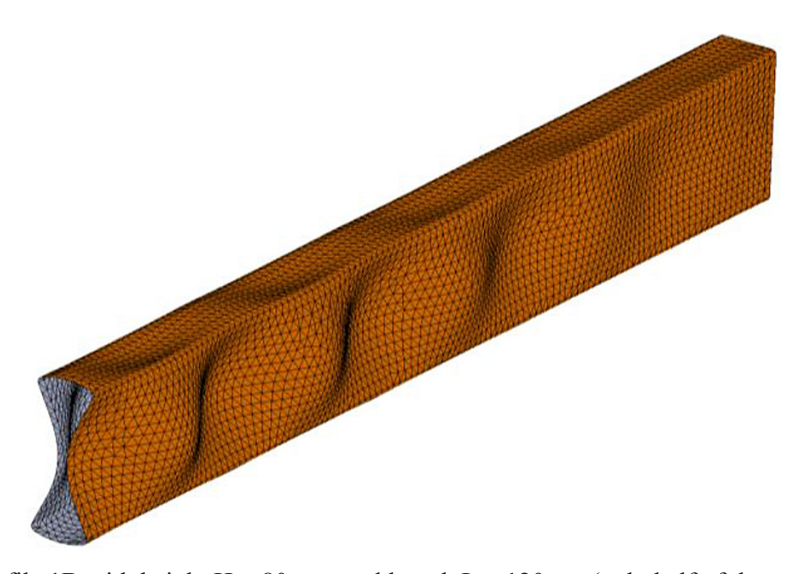


Figure 31. Profile 1B with height H = 80 mm and length L = 120 cm (only half of the profile is shown): buckling form ($F_{cr} = 35.5 \text{ kN}$)

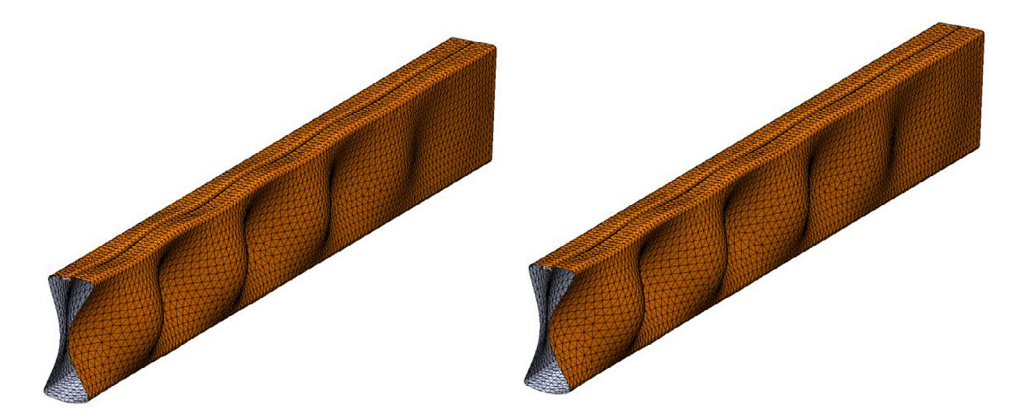


Figure 32. Profile 1A with height H = 80 mm and length L = 120 cm (only half of the profile is shown): buckling form with no bond at the bend ($F_{cr} = 39.6 \text{ kN}$) and with full bond at the bend ($F_{cr} = 40.0 \text{ kN}$)

of profiles 1A and 1B and the critical force for 120 cm long beams compressed axially is shown in Figure 36. This figure shows that cold-formed profiles, regardless of the way of modeling the bend, are less susceptible to loss of stability during axial compression. Although their advantage over standard rectangular profiles decreases with the length of the beam.

In the case of 1A profiles with height H = 120 mm, in the entire considered length range, the beam in which the bend is made correctly and does not split, only undergoes local buckling. The critical force in this case is 24.1 kN and practically does not depend on the length of the profile. It is about 9% greater than the critical force of a standard rectangular profile of the same dimensions.

The critical force of profile 1A with a height of H = 200 mm in the considered range is about

5% greater than the critical force of profile 1B provided that full bonding is assumed at the bend. In the case of no bonding, the critical force of profile 1A is about 2.5% less than the critical force of profile 1B. Moreover, in the considered length range, i.e. from 120 to 240 cm, the critical force of profiles 1A and 1B with a height of 200 mm is independent of the beam length.

CONCLUSIONS

The first part of this paper presents an analysis of the stability of thin-walled channel sections in the state of pure bending. First, it is shown that stiffening the edges of the flanges with single and double bends increases the load capacity of the profiles. This is not so much due to the fact that



Figure 33. Profile 1A with height H = 80 mm and length L = 150 cm (only half of the profile is shown): buckling form with no bond at the bend ($F_{cr} = 37.5 \text{ kN}$)

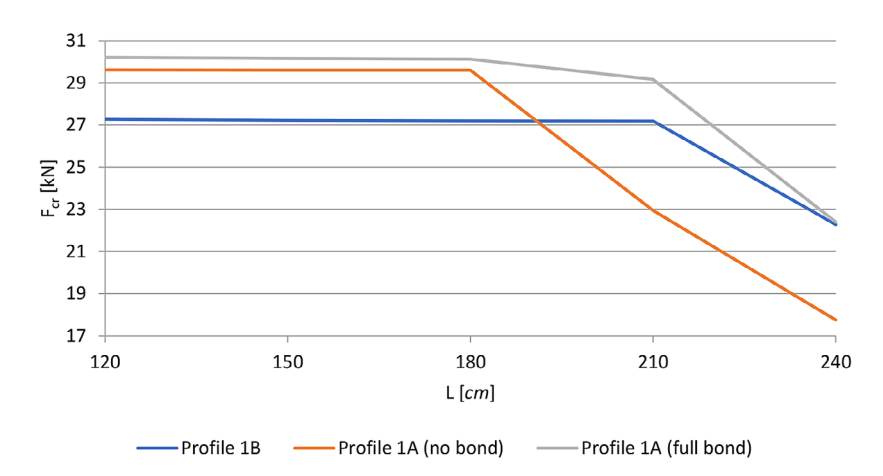


Figure 34. Comparison of critical forces of profiles 1A and 1B, H = 100 mm

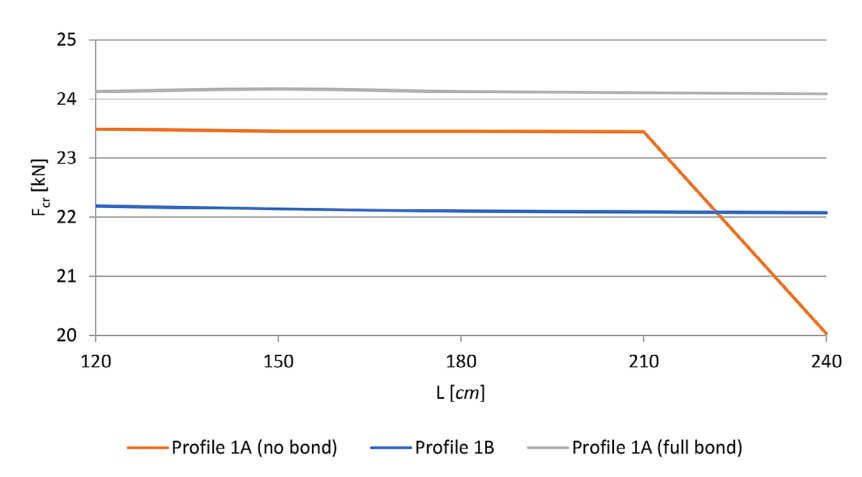


Figure 35. Comparison of critical forces of profiles 1A and 1B, H = 120 mm

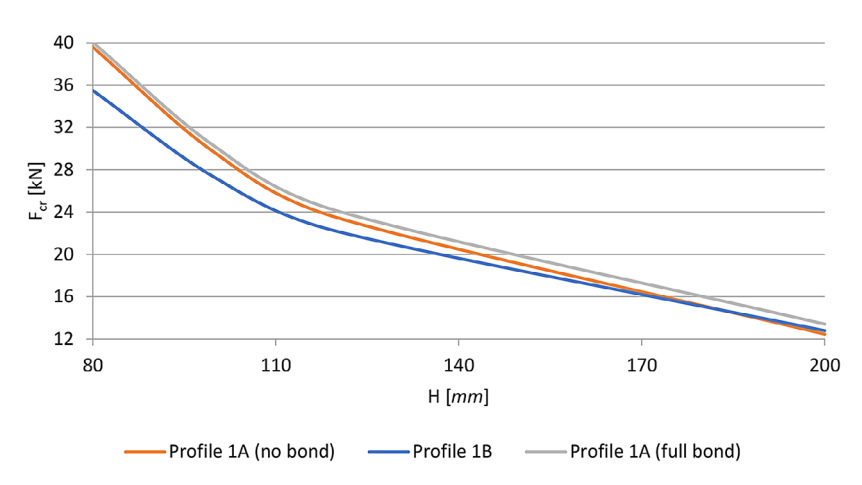


Figure 36. Relationship between critical force and height of profiles 1A and 1B with length L = 120 cm

the cross-section of the beams is increased, or the moments of inertia of the cross-section (bending strength coefficients), but rather due to the increased values of critical stresses. The upper/compressed flange in a classic cold-formed channel section is exposed to local loss of stability. In

the case of short beams, even reducing the length of the beam or the distance between the supports does not increase the value of critical stresses. Only stiffening the edge of the flange with a single or double bend in the considered cases solves the problem of local loss of stability. It should also be noted that the values of critical stresses of a beam with a double bend are about 42% higher than in the case of a beam with a single bend, and this with only 18% greater mass. Comparing the double-bend beam to the classic cold-formed channel section is even more favourable, as its critical stresses are about 170–180% higher than those of the only 40% lighter channel section.

These considerations show that open thinwalled profiles are interesting structural elements. Their production from thin sheets of galvanized sheet metal and cold processing eliminate the need for additional protection of finished elements. Moreover, even local damage to the protective layer does not lead to steel corrosion thanks to cathodic protection. These profiles may be exposed to a loss of stability: local, distortional or global. However, proper design of the cross-sectional shape of the profile and stiffening of the elements exposed to a loss of stability solve this problem, especially in relatively short beams. It is also significant that thanks to the use of cold bending technology, the dimensions of the cross-section can be adjusted to individual applications. Detailed parameters of stiffening bends can be selected through parametric optimization depending on specific needs.

In the second part of this study, standard rectangular profiles were compared with the proposed thin-walled cold-formed profiles. Thanks to the special shape of the bend, although they are not welded along the joint edge, they can be treated as closed profiles. In this way, profiles of any dimensions can be obtained, without the limitations resulting from the series of types available in steelworks. In addition, this method can be used to produce profiles with relatively large cross-sectional dimensions and small wall thickness. In order to assess the suitability of these profiles, their stability was compared. The critical force of thin-walled profiles compressed axially is greater than that of their standard, closed counterparts, but on condition that the bend strength is sufficient to prevent the profile from "tearing apart". Appropriately high and short thin-walled profiles losing stability due to local wall buckling are more resistant to loss of stability than standard rectangular profiles, even if the bend strength is low.

In summary, thin-walled, cold-formed rectangular cross-section profiles are an interesting alternative to standard rectangular profiles. If they are made correctly and the durability of the connection at the bending point is ensured, the stability of thin-walled profiles is higher than their standard counterparts.

Acknowledgements

The project was funded by the National Science Centre, Poland allocated on the basis of the decision No. DEC-2021/43/B/ST8/00845 of 2022-05-23 — Contract No. UMO-2021/43/B/ST8/00845. Project No. WND-RP-PD.01.02.01-20-0019/16 entitled, "Establishment of a Research and Development Center and Conducting Industrial Research Focused on Optimizing Thin-Walled Sheet Metal Structural Elements and Developing Efficient Manufacturing Technologies" carried out under contract No. UDA-RP-PD.01.02.01-20-0019/16-00 dated 24.08.2017.

REFERENCES

- Hancock GJ. Cold-formed steel structures. J Constr Steel Res. 2003;59(4):473–87, https://doi.org/10.1016/s0143-974x(02)00103-7
- 2. Rhodes J, Seah LK. Buckling of edge-stiffened thin-walled beam sections. Proc Inst Civil Eng-Struct Build. 1992;94(3):323–34, https://doi.org/10.1680/istbu.1992.20292
- 3. Laudiero F, Zaccaria D. Finite-element analysis of stability of thin-walled-beams of open section. Int J Mech Sci. 1988;30(8):543–57, https://doi.org/10.1016/0020-7403(88)90098-7
- 4. Koczubiej S, Cichon C. Global static and stability analysis of thin-walled structures with open cross-section using FE shell-beam models. Thin-Walled Struct. 2014;82:196–211, https://doi.org/10.1016/j. tws.2014.04.014
- Adany S, Schafer BW. Buckling mode decomposition of single-branched open cross-section members via finite strip method: Derivation. Thin-Walled Struct. 2006;44(5):563–84, https://doi.org/10.1016/j.tws.2006.03.013
- Pawlak AM, Paczos P. Analysis of strength and resistance to loss of stability of thin-walled channel columns with non-standard cross-sectional shape.
 Arch Civ Eng. 2024;70(3):101–16, https://doi.org/10.24425/ace.2024.150973
- Pawlak AM, Górny TA, Plust M, Paczos P, Kasprzak J. Imperfections in thin-walled steel profiles with modified cross-sectional shapes - Current state of knowledge and preliminary studies. Steel Compos Struct. 2024;52(3):327–41, https://doi. org/10.12989/scs.2024.52.3.327

- 8. Machado SP. Non-linear stability analysis of imperfect thin-walled composite beams. Int J Non-Linear Mech. 2010;45(2):100–10, https://doi.org/10.1016/j.ijnonlinmec.2009.09.006
- Magnucka-Blandzi E. Effective shaping of coldformed thin-walled channel beams with doublebox flanges in pure bending. Thin-Walled Struct. 2011;49(1):121–8, https://doi.org/10.1016/j. tws.2010.08.013
- Magnucka-Blandzi E, Paczos P, Wasile-wicz P. Buckling study of thin-walled channel beams with double-box flanges in pure bending. Strain. 2012;48(4):317–25, https://doi.org/10.1111/j.1475-1305.2011.00825.x
- 11. Jasion P, Pawlak A, Paczos P. Buckling and postbuckling behaviour of selected cold-formed C-beams with atypical flanges. Eng Struct. 2021;244:13, https://doi.org/10.1016/j.engstruct.2021.112693
- 12. SudhirSastry YB, Krishna Y, Budarapu PR. Parametric studies on buckling of thin walled channel beams. Comput Mater Sci. 2015;96:416–24, https://doi.org/10.1016/j.commatsci.2014.07.058
- Basaglia C, Camotim D, Silvestre N. Post-buckling analysis of thin-walled steel frames using generalised beam theory (GBT). Thin-Walled Struct. 2013;62:229–42, https://doi.org/10.1016/j. tws.2012.07.003
- 14. Basaglia C, Camotim D, Silvestre N. Global buckling analysis of plane and space thin-walled frames in the context of GBT. Thin-Walled Struct. 2008;46(1):79–101, https://doi.org/10.1016/j. tws.2007.07.007
- Grenda M, Paczos P. Experimental and numerical study of local stability of non-standard thin-walled channel beams. J Theor Appl Mech. 2019;57(3):549– 62, https://doi.org/10.15632/jtam-pl/109601
- 16. Bourihane O, Ed-Dinari A, Braikat B, Jamal M, Mohri F, Damil N. Stability analysis of thin-walled beams with open section subject to arbitrary loads. Thin-Walled Struct. 2016;105:156–71, https://doi.org/10.1016/j.tws.2016.04.008
- 17. Martins AD, Camotim D, Gonçalves R, Dinis PB. On the mechanics of local-distortional interaction in thin-walled lipped channel columns. Thin-Walled Struct. 2018;125:187–202, https://doi.org/10.1016/j.tws.2017.12.029

- 18. Lofrano E, Paolone A, Ruta G. A numerical approach for the stability analysis of open thin-walled beams. Mech Res Commun. 2013;48:76–86, https://doi.org/10.1016/j.mechrescom.2012.12.008
- 19. Chu XT, Ye ZM, Li LY, Kettle R. Local and distortional buckling of cold-formed zed-section beams under uniformly distributed transverse loads. Int J Mech Sci. 2006;48(4):378–88, https://doi.org/10.1016/j.ijmecsci.2005.11.005
- Li YL, Li YQ, Shen ZY. Investigation on flexural strength of cold-formed thin-walled steel beams with built-up box section. Thin-Walled Struct. 2016;107:66– 79, https://doi.org/10.1016/j.tws.2016.05.026
- 21. Pastor MM, Roure F. Open cross-section beams under pure bending II. Finite element simulation. Thin-Walled Struct. 2009;47(5):514–21, https://doi.org/10.1016/j.tws.2008.10.021
- 22. Horacek M, Melcher J, editors. Lateral Torsional Buckling of Thin-Walled Cold-Formed Steel Beams with Web Holes - Finite Element Analysis. International Conference on Materials Science and Mechanical Engineering (ICMSME 2013); 2013 Oct 27-28; Kuala Lumpur, MALAYSIA. STAFA-ZU-RICH: Trans Tech Publications Ltd; 2014.
- 23. Kim NI, Shin DK, Park YS. Coupled stability analysis of thin-walled composite beams with closed cross-section. Thin-Walled Struct. 2010;48(8):581–96, https://doi.org/10.1016/j.tws.2010.03.006
- 24. Niu RT, Gao WC, Liu W. Effect of moment of inertia on elastic stability of rectangular webs for thinwalled beams under a transverse load. Thin-Walled Struct. 2014;85:34–41, https://doi.org/10.1016/j. tws.2014.07.019
- 25. Kesti J, Davies JM. Local and distortional buckling of thin-walled short columns. Thin-Walled Struct. 1999;34(2):115–34, https://doi.org/10.1016/s0263-8231(99)00003-8
- 26. Zhao O, Rossi B, Gardner L, Young B. Behaviour of structural stainless steel cross-sections under combined loading - Part I: Experimental study. Eng Struct. 2015;89:236–46, https://doi.org/10.1016/j. engstruct.2014.11.014
- 27. Gardner L, Yun X. Description of stress-strain curves for cold-formed steels. CONSTRUCTION AND BUILDING MATERIALS. 2018;189:527–38, https://doi.org/10.1016/j.conbuildmat.2018.08.195